JOURNAL OF MATERIALS SCIENCE 32 (1997) 3001–3006

Transparent conducting lithium-doped nickel oxide thin films by spray pyrolysis technique

P. PUSPHARAJAH, S. RADHAKRISHNA
Institute of Advanced Studies, University of Malaya, 50603 Kuala Lumpur, Malaysia

A. K. AROF
Physics Division, Centre for Foundation Studies in Science, University of Malaya, 50603 Kuala Lumpur, Malaysia

Nickel oxide (NiO) and lithium-doped nickel oxide films were deposited by the spray pyrolysis technique using $NiCl_2$ and LiCl as starting materials. All the films were greenish-grey in colour and confirmed by X-ray analysis. The best NiO films were obtained when the substrate temperature, $T_s = 480\,^{\circ}C$ where a conductivity of $2.1 \times 10^{-1}\,\Omega^{-1}\,cm^{-1}$ and transparency above 80% in the visible region are achieved. High transparency (above 80%) and highly conducting NiO films were obtained when doped with lithium.

1. Introduction

NiO is a candidate for p-type transparent conducting films with a band gap energy from 3.6 to 4.0 eV [1]. Although stoichiometric NiO is an insulator with a resistivity of the order of $10^{13}\,\Omega\,cm$ at room temperature, its resistivity can be lowered by an increase of Ni^{3+} ions resulting from an addition of monovalent atoms such as lithium or by the appearance of nickel vacancies and/or interstitial oxygen in NiO crystallities [1, 2]. Transparent conducting nickel oxide films have a wide range of applications in optoelectronic and thermal devices. In the area of optoelectronics, nickel oxide is well known as an electrochromic material [3, 4]. Another area where NiO films are of great interest is in the new optical recording material of a Ni–NiO heterogeneous system that would realize a portable medium by using a laser diode beam for recording and reading. The new medium using a thin film of Ni–NiO needs no protecting layer because of its stability under usage. This material has advantages over conventional materials such as tellurium which is easily oxidizable in high humidity [5].

There have been reports on nickel oxide films produced by sputtering [2–5], by electron beam evaporation [6] and by dip coating [7]. A resistivity as low as $1.4 \times 10^{-1}\,\Omega\,cm$ and a hole concentration of the order of $10^{19}\,cm^{-3}$ were obtained by radio frequency (r.f.) magetron sputtering. For a film of thickness 110 nm an average transmittance of about 40% was reported in the visible range [2]. Varkey and Fort [7] have deposited insulating NiO films of 80 nm thickness using the dip technique. An average transmittance of about 80% in the visible range and a band gap of 4.0 eV were reported for the film produced using this technique.

2. Sample preparation

The nickel oxide and lithium-doped nickel oxide films were prepared using the spray pyrolysis deposition technique. Nickel chloride and lithium chloride were used as the starting materials. The spraying solution consists of 2 g of starting material, dissolved in a mixture of ethyl alcohol and water with the volume ratio of 3:1, respectively, which gives a total volume of 10 ml.

After spraying, the films were removed immediately from the spraying chamber and allowed to cool in air at room temperature to freeze the oxidation state. Physical properties of the films were studied at different substrate temperature, T_s, nozzle–substrate distance, D_{sn}, solution flow rate, F_r and lithium concentrations. Further details of the experimental methods are found in our earlier papers [8, 9].

3. Results and discussion

NiO films prepared by spray pyrolysis of $NiCl_2$ solution were initially (all the films) yellowish in colour and became clear after cooling to room temperature. At lower substrate temperatures (below 350 °C), the films were physically unstable. These films absorb water molecules from the air and form a watery surface. At temperatures above 350 °C, the physical stability and adhesiveness to the substrate improves. Cloudy greenish-grey films were obtained for films deposited at substrate temperatures above 450 °C. X-ray analysis shows that NiO films deposited by spray pyrolysis are amorphous.

Fig. 1 shows scanning electron microscopy (SEM) micrographs of the NiO films prepared at substrate temperatures of 350 and 400 °C. It can be observed that the droplets are uniformly distributed throughout

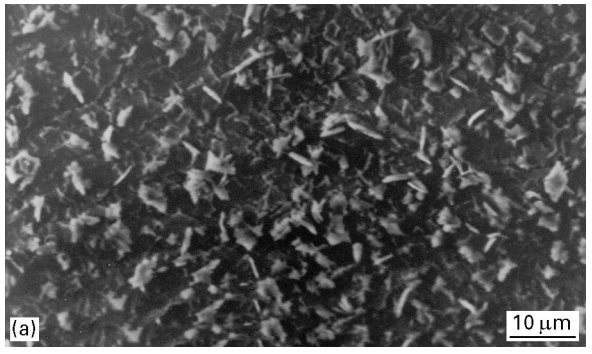

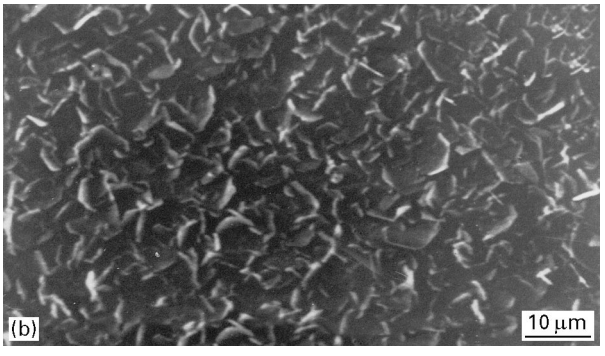

Figure 1 SEM micrograph of NiO films obtained at (a) $T_s = 300\,^{\circ}C$ and (b) $T_s = 400\,^{\circ}C$.

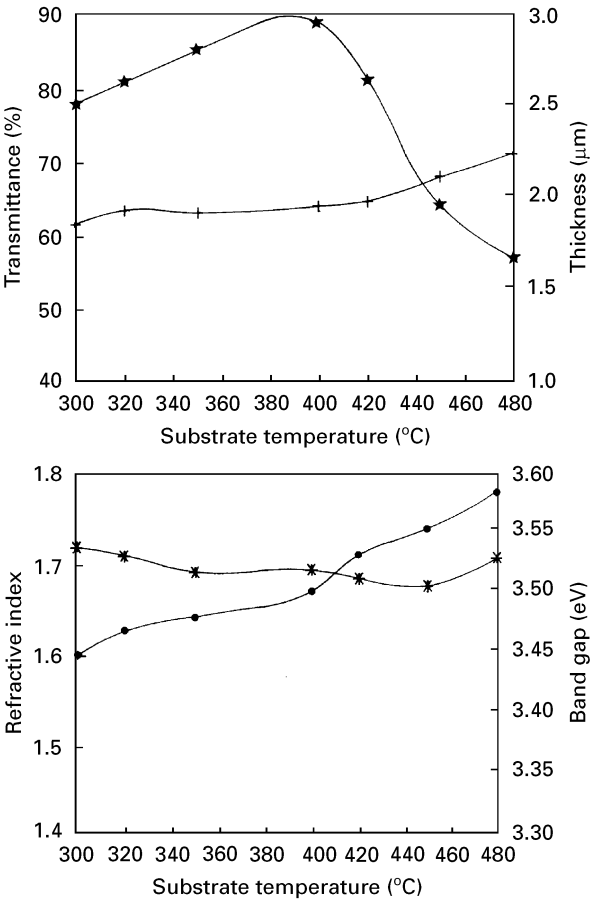

Figure 2 Variation of transmittance (★), thickness (+), refractive index (●) and band gap (*) with substrate temperature, T_s.

the films. Grain size is influenced by the substrate temperature, T_s. From the micrographs it is observed that large grains can be obtained by depositing at higher T_s. This is because when the substrate temperature is increased, the mobility of the molecules on the surface is improved and causes an increase in grain size.

Microchemical analysis of the NiO film by electron dispersive spectroscopy (EDAX) shows the decrease in chlorine content in the films as the substrate temperature is increased. This shows that at low temperatures only partial conversion of $NiCl_2$ to NiO takes place. The conversion of $NiCl_2$ to NiO increases with increasing substrate temperature.

The optical transmission of NiO films in the wavelength range of 290–800 nm for different substrate temperatures, T_s, is shown in Fig. 2. Transparency of the film decreases with increasing substrate temperature. Above 450 °C, the films turned greenish-grey and cloudy [7]. The average transmission of very cloudy films have been observed to be as low as 40%. High transmittance in the visible region of the spectrum at lower T_s suggests the possible use of these films as glazing materials [2].

Extrapolation of the linear portion of the transmittance curve to zero absorbance (100% transmission) shows that the NiO films have an optical band gap between 3.15–3.50 eV. Bulk crystalline NiO has a band gap of $\sim$4.0 eV [1, 2], much higher than the value obtained for sprayed films. The difference could be mainly due to the amorphous structure. In amorphous materials the electron transitions may be either from localized states in the conduction band or from extended states in the valence band to localized states at the conduction edge [10]. This leads to lower energies than those for polycrystalline or bulk crystalline materials.

The transmission, refractive index, film thickness and band gap of the NiO films are shown in Fig. 3 for samples prepared at various nozzle–substrate distances. It can be observed that in general an increase in nozzle–substrate distance improves the transmission up to a nozzle–substrate distance of 29 cm beyond which transmission begins to decrease and significantly falls off beyond a nozzle–substrate distance of 30 cm. This improvement may be attributed to the decrease in the band gap, which is observed to decrease from $\approx$ 2.85 eV for the sample prepared at a nozzle–substrate distance of 26 cm to $\approx$ 2.50 eV for the sample prepared at a nozzle–substrate distance of 29 cm. At nozzle–substrate distances greater than 29 cm, the band gap is observed to increase and it increases significantly to $\approx$3.70 eV when the transmission falls off significantly to just above 20% at a nozzle–substrate distance of 34 cm.

Fig. 4 shows the relationship between the transmittance, film thickness, refractive index and band gap with the flow rate, F_r. It can be observed that transmittance does not vary much as the solution flow rate is doubled from 8 to 16 ml min^{-1}. From the same figure it can be seen that the film thickness increases by about 20% as F_r is doubled. The increase in thickness of NiO films may be understood by considering the deposition rates. The deposition rate, R, depends on

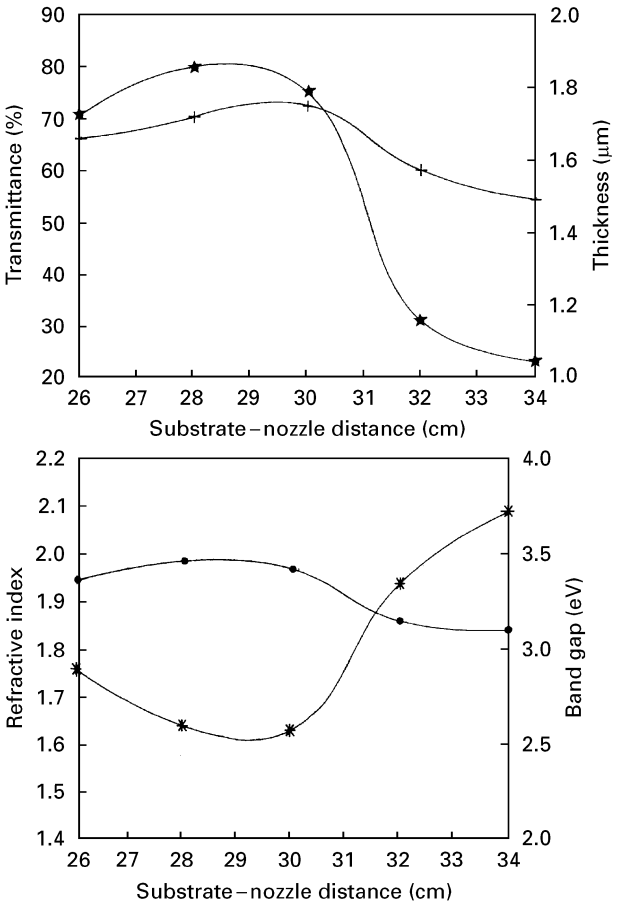

Figure 3 Variation of transmittance (★), thickness (+), refractive index (●) and band gap (*) with nozzle–substrate distance, D_{sn}.

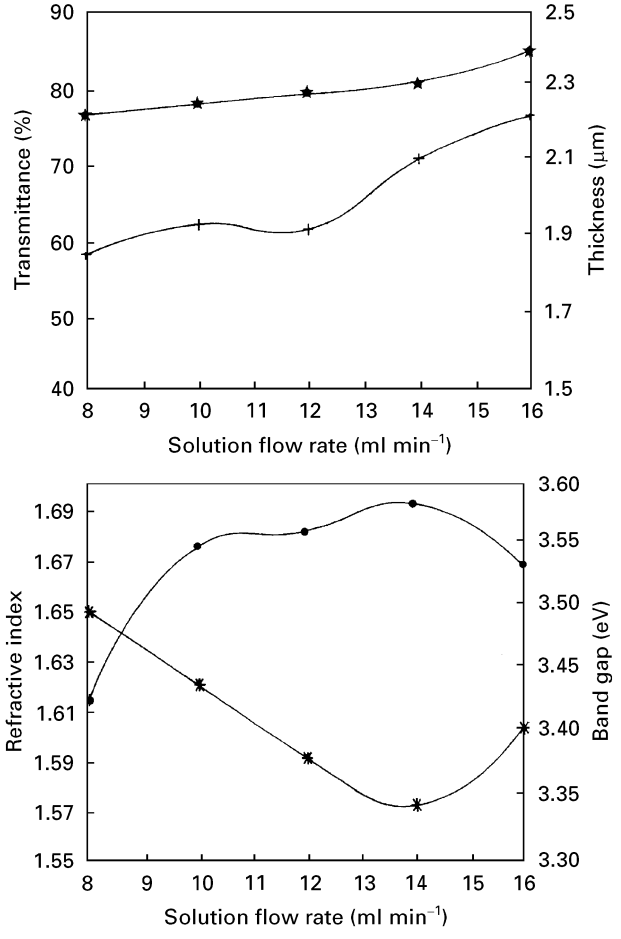

Figure 4 Variation of transmittance (★), thickness (+), refractive index (●) and band gap (*) with solution flow rate, F_r.

the mass transfer coefficient, K_g, the diffusion potential, ΔY, the molecular weight, M, and the density, ϕ, of the starting material [11]:

$$R = (M/\phi)K_g\Delta Y$$

The increase in solution flow rate increases the deposition rate which leads to the increase in thickness but does not affect the transparency of the film, since the variation in transparency is less than 10%. The small variation in transparency can be understood from the small variation in refractive index and possibly to the lower refractive index of the sample (compare refractive index values in Figs 3 and 4) obtained as the solution flow rate is doubled. The reciprocal relation between transmittance and band gap is once again demonstrated although the variation of these parameters with the solution flow rate is quite small.

Fig. 5 shows variation of transmission, optical constant, film thickness and band gap with lithium concentration. Lithium-doped films show high transparency throughout the visible region with average transmission above 80%. With increasing lithium concentration, the film thickness is observed to decrease. This can be attributed to the displacement of Ni atoms by Li atoms which are smaller than Ni atoms. Differences in orientation of the Ni, Li and O atoms may result in slightly thicker films for samples doped with higher Li concentrations. Since the transparency of the films is quite constant for different Li concentrations, the refractive index also does not show much variation with Li concentration.

Resistivity was measured at room temperature for all the films. The dependence of resistivity as a function of substrate temperature for nickel oxide films is shown in Fig. 6. The film resistivity decreases with increasing substrate temperature. The decrease can be due to either a kinetic reaction in the deposition process or to the increase in film thickness. At higher substrate temperatures, the droplets will absorb more thermal energy such that all the solvent will vaporize just before reaching the substrate and approach homogeneous to heterogeneous reaction conditions. This heterogeneous reaction reported in [12] will improve the growth rate and the carrier density.

The variation in resistivity, ρ, with D_{sn} (Fig. 7) for the NiO films also suggests that with increasing D_{sn} there is the possibility of a change from a homogeneous reaction to a heterogeneous reaction. At lower D_{sn} (up to 30 cm), the resistivity is low and shows a small increase with increasing D_{sn}. On increasing D_{sn}, the droplet travels a greater distance in the pyrolytic zone such that all the solvent will be vaporized and decomposition of nickel oxide will occur at the surface of the substrate. Under this condition it approaches a hetereogeneous reaction. Since the droplet travels much greater distance in the furnace, it will absorb more heat and the decomposition may occur in the gas phase itself, thus affecting the growth rate. This has an effect on the film thickness and increases the resistivity 10 times higher than D_{sn} at 30 cm. This result is quite consistent with that shown in Fig. 3, where, for D_{sn} greater than 30 cm, the film thickness of the samples is observed to decrease.

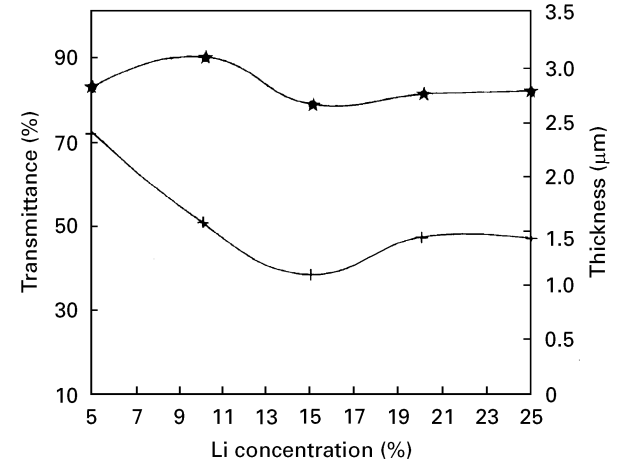

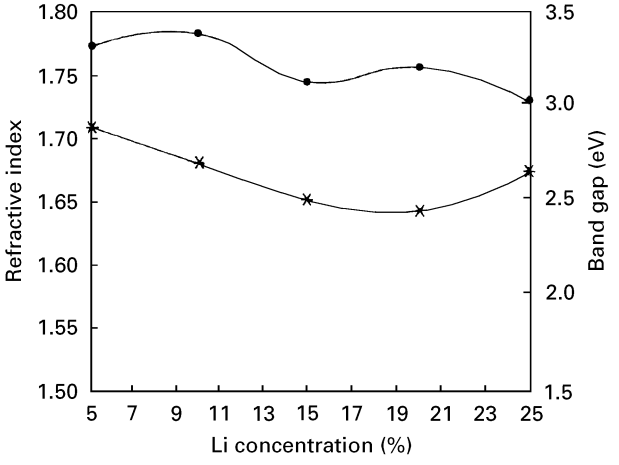

Figure 5 Variation of transmittance (★), thickness (+), refractive index (●) and band gap (*) with lithium concentration.

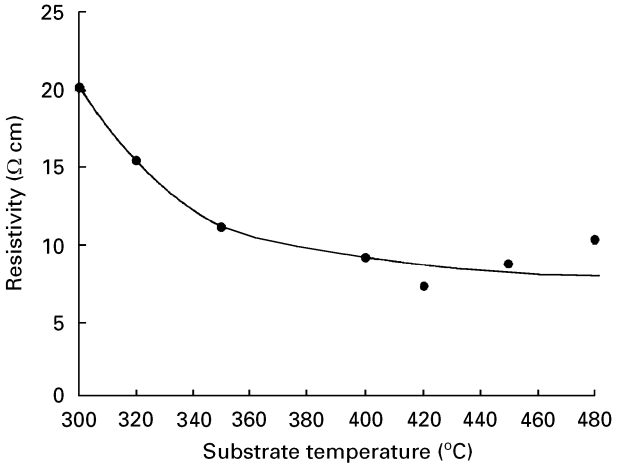

Figure 6 Variation of electrical resistivity of NiO film with substrate temperature, T_s.

Fig. 8 shows resistivity, ρ, of NiO films at different solution flow rates, F_r. The resistivity decreases with F_r and at a flow rate 16 ml min^{-1}, the resistivity is 8.3 Ω cm. This improvement can be attributed to the increase in thickness, as shown in Fig. 4.

The conduction in nickel oxide is due to the presence of Ni^{3+} ions [1, 2]. These ions may be formed either by the appearance of NiO nickel vacancies or by

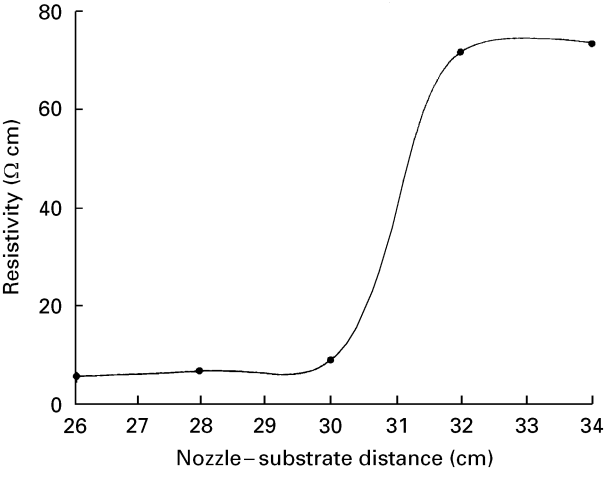

Figure 7 Variation of electrical resistivity of NiO film with substrate–nozzle distance, D_{sn}.

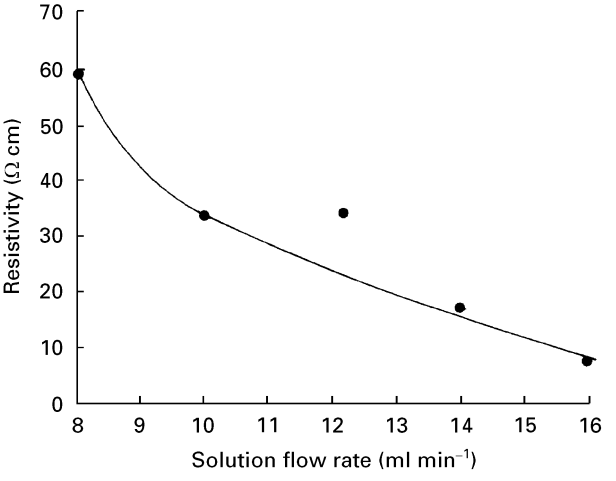

Figure 8 Variation of electrical resistivity of NiO film with solution flow rate, F_r.

the incorporation of monovalent atoms. Introduction of Li^+ into the NiO films gives rise to acceptor centres Li^+–Ni^{3+}. At low temperatures, the Ni^{3+} holes formed in this way are bound to a lithium ion, which has an effective negative charge. At higher temperatures these holes can detach from the Li^+–Ni^{3+} centres and move quasi-freely in the sample by exchange of electrons between Ni^{3+} and adjacent Ni^{2+} ions [1].

The variation in resistivity with the lithium concentration is shown in Fig. 9. The resistivity of the films shows a minimum value of 0.7 Ω cm at 25% of lithium concentration. The decrease in resistivity of Li-doped NiO film depends mainly on the increase in the number of Ni^{3+} ions and possibly to the overall decrease in band gap as the Li concentration increases from 5 to 25%.

The electrical properties of NiO films depend largely on their structure and composition, and consequently on the deposition environment. The impedance was measured and analysed in the complex plane for various parameters which assist in obtaining a deep insight into the mechanism controlling the conductivity of the NiO material in thin film form. Impedance spectroscopy was carried out for the amorphous NiO sample in the frequency range

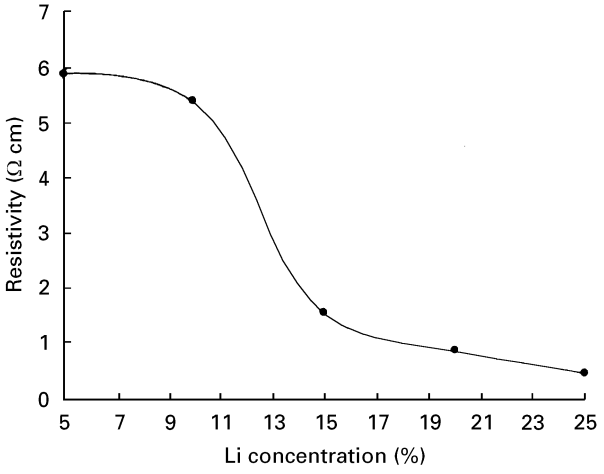

Figure 9 Variation of electrical resistivity of NiO film with lithium concentration.

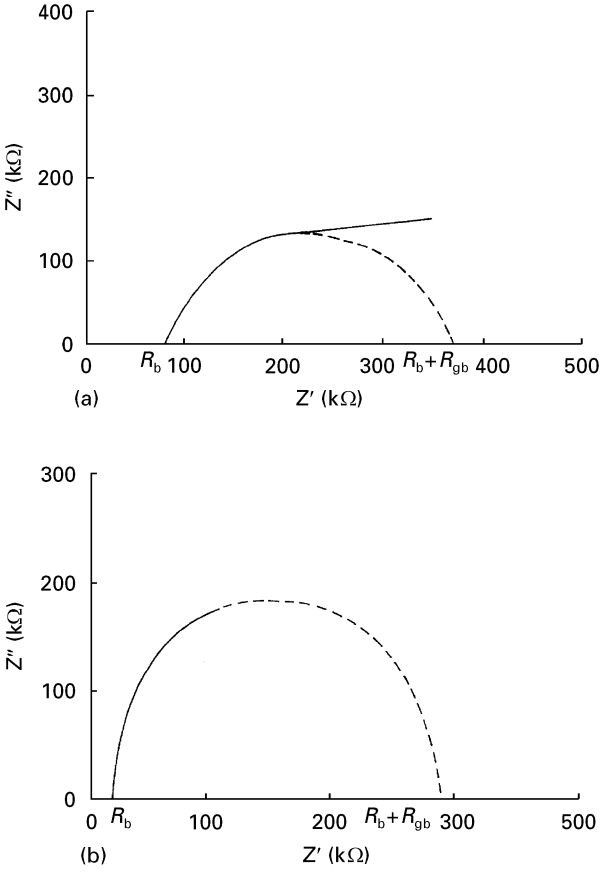

Figure 10 A.c. conductivity curves of NiO films prepared at (a) $T_s = 300\,^{\circ}C$ and (b) $T_s = 400\,^{\circ}C$.

between 40 Hz to 100 kHz at room temperature to obtain the real and imaginary impedances. The plot of imaginary impedance versus real impedance may take the shape of a semicircle which ends at the origin of the imaginary impedance and real impedance axes. If this is the case, then the intercept of the plot at the lower frequency end will give the bulk resistance, R_b. In the case where two semicircles can be observed, the intercept of the second semicircle with the real impedance axis (furthest from the origin) will give the value of $R_b + R_{gb}$, where R_{gb} is the grain boundary resistance. Figs 10 and 11 show the complex impedance

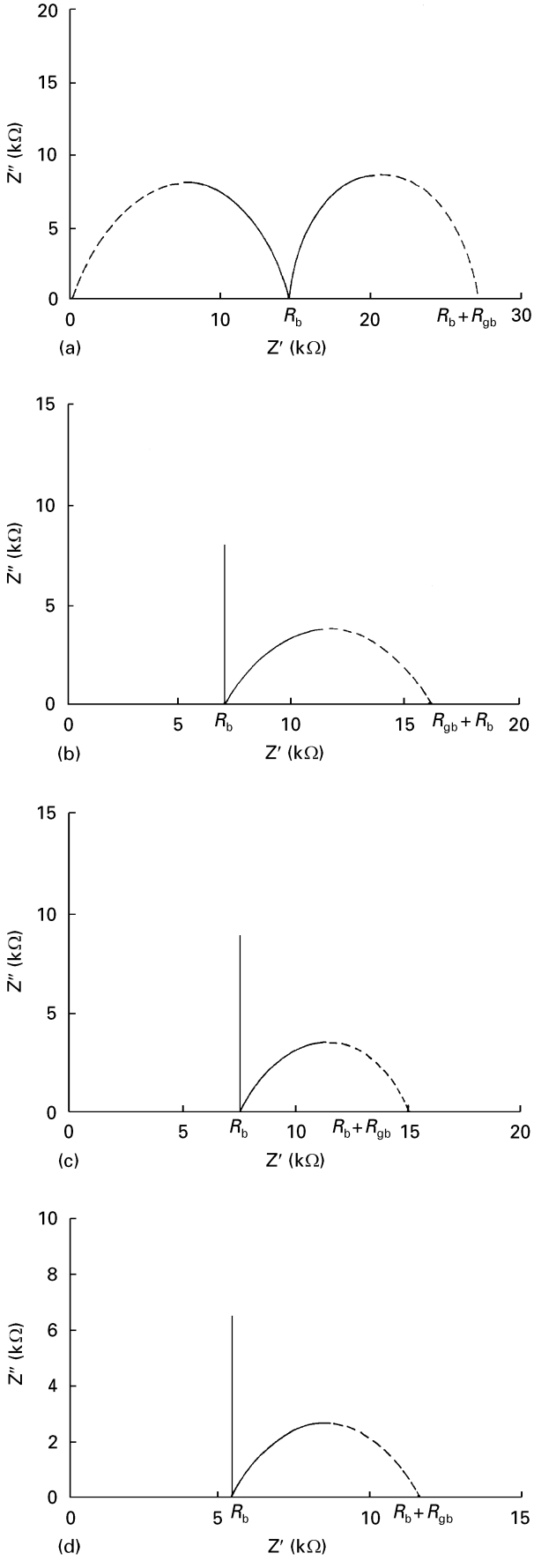

Figure 11 A.c. conductivity curves of lithium doped NiO films prepared at (a) 5%, (b) 10%, (c) 15% and (d) 20% lithium concentration.

plots for some of the NiO films. Extrapolating the high and low frequency limits of the arcs, the plots intercept the real axis (Z') at resistance values of R_b

and $R_b + R_{gb}$, respectively. For all the substrate temperatures, the NiO films show a single semicircle with R_b and $R_b + R_{gb}$ at the real axis intercepts. The decrease in R_b and R_{gb} with substrate temperature may be attributed to the growth of the film. Knowing R_b, the resistivity of the films can be calculated from the equation $p = R_b A/l$ where A is the surface area of the sample and l its distance between electrodes.

Fig. 11 shows the Cole–Cole plot of NiO films at different lithium, concentrations. Semicircles intercepting the real impedance axis at R_b and $R_b + R_{gb}$ were obtained for all the films. For films with 5% lithium concentration another semicircle which intercepts the real axis at the origin and R_b is expected. This semicircle is due to a parallel combination of the bulk resistance, R_b, and the bulk capacitance, C_b, of the sample. The conduction mechanism of this sample is ruled by two parallel R–C circuits [13]. Films with more than 5% lithium concentration do not show the dependence of the real part of impedance with frequency after the bulk resistance but the imaginary part of impedance shows an abrupt change with frequency. For these samples, the conduction mechanism may be controlled in the same way as that of an equivalent circuit comprising a serial combination of a resistor with resistance R_b and a capacitor with capacitance C_b in series with a parallel R–C circuit where the resistance is R_{gb} and capacitance is C_{gb}.

4. Conclusions

Highly transparent and well conducting amorphous thin films of NiO and lithium-doped NiO have been prepared by the spray pyrolysis technique. Films obtained by this method are adherent and have a uniform surface. NiO films have been prepared with resistivities as low as 5 Ω cm and with almost 90% transmission in the visible spectrum for 2 μm thick films and the conductivity is reasonably stable when samples are stored at room temperature. From the Cole–Cole plot we can conclude that the resistance of lithium-doped NiO films do not show any dependence on frequency in the high frequency range. NiO and lithium-doped NiO films fabricated by spray pyrolysis should be useful as a less expensive p-type transparent electrode for solar cells and displays.

References

1. Z. M. JARZEBSKI, "*Oxide Semiconductors*" (Pergamon Press, Poland, 1973).
2. H. SATO, T. MINAMI, S. TAKATA and Y. YAMADA, *Thin Solid Films* **236** (1993) 27
3. J. S. E. M. SVENSON and C. G. GRANQVIST, *Appl. Phys. Lett*. **49** (1986) 1566.
4. SHOJI YAMADA, TATSUO YOSHIOKA, MASATOSHI MIYASHITA, KAZUO URABE and MICHIHIKO KITAO, *J. Appl. Phys.* **63** (1988) 2116.
5. ATSUKO IIDA and REIJI NISHIKAWA, *Jpn. J. Appl. Phys.* **33** (1994) 3952.
6. P. LUNKENHEIMER, A. LOIDL, C. R. OTTERMANN and K. BANGE, *Phys. Rev. B* **44** (1991) 5927.
7. A. J. VARKEY and A. F. FORT, *Thin Solid Films* **235** (1993) 47.
8. P. PUSPHARAJAH, A. K. AROF and S. RADHAKRISHNA, *J. Phys. D*: *Appl. Phys.* **27** (1994) 1518.
9. P. PUSPHARAJAH and S. RADHAKRISHNA, *Jur. Sains* **2** (1994) 195.
10. A. F. AKTARUZZAMAN, G. L. SHARMA and L. L. MALHOTRA, *Thin Solid Films* **198** (1991) 67–74
11. V. VASU and A. SUBRAHMANYAM, *Thin Solid Films* **193/194** (1990) 973.
12. *Idem*, *ibid*. **193/194** (1990) 696.
13. S. CHANDRA, "Superionic Solids: *Principle and Applications*" (North-Holland, Amsterdam, 1981).

Received 3 January
and accepted 19 November 1996